

Acceptance testing of a large aperture dynamic wavefront sensor

David J. Fischer*, Alan Wertheimer, Laurie Hill
Eastman Kodak Company, 1447 St. Paul St, Rochester, NY 14653

ABSTRACT

A large aperture dynamic wavefront sensor (WFS) was tested and qualified for use against its design requirements. As the WFS was designed to measure the relative slope of dynamic wavefronts, the test system created dynamic wavefronts, moving at 35 Hz to 315 Hz, with slopes on the order of 50 nanoradians. The essential test system was an f/2.3 parabolic mirror with a laser source at the focal point, offset laterally by a fold mirror. The reflected light was nominally collimated and incident on the WFS at zero degrees. The source hardware was mounted on two crossed-translation stages that could drive a 540 μm , 1/2 Hz trapezoidal motion, inducing tilt in the collimated beam. This 100 μR wavefront modulation calibrated the WFS. The fold mirror was mounted on a PZT which oscillated the fold mirror from 35 Hz to 315 Hz at tilt angles near 10 μR . This tilt moved the virtual source point, inducing wavefront tilts in the collimated output beam on the order of 100 nR. These fast, very small wavefront tilts were used to test the WFS performance. The test system, procedure, and calibration procedures are described.

Keywords: optical, metrology, dynamic, wavefront, sensor

1. INTRODUCTION

A large (2.4 meter diameter) wavefront sensor (WFS)¹, built for Kodak by Optical Physics Company (OPC) arrived at Kodak in December, 2003 and was tested with a full aperture parabola in January/February, 2004. The WFS is designed to measure wavefront changes in the 10 to 600 Hz range, using monochromatic laser light of 0.852-microns wavelength.

The goal of the WFS test was to characterize the WFS performance over all 448 sub-apertures in the 1 to 50 nR range at approximately 10 to 200 Hz. The results were encouraging but incomplete due to the failure of a seismic isolation system attached to the WFS, a lack of seismic isolation of the parabola, and uncalibrated WFS alignment sensors. Sinusoidal tilt signals of 70 nR (peak-to-valley) at various temporal frequencies between 35 Hz and 315 Hz were clearly reported by the WFS. Input signals in the 12 nR range were also identified in the data. However, low frequency seismic disturbances, particularly in the 2 to 10 Hz range, created simultaneous tilt signals in the 100 to 1000 nR range, making it impossible to test the WFS to its performance limits. A retest is planned for August 2004. This report describes the results of the first test with lessons learned and recommendations for the second test.

2. TEST PRINCIPLES

The WFS test is a calibration and verification process for the WFS. Because the WFS is required to measure relative wavefront tilts in motion at rates from 10Hz to 400 Hz down to a five nano-radian (nR) accuracy, the test system must create such signals. The test concept, sketched in Fig. 1, is to dynamically tilt a collimated beam by moving the source beam laterally about its nominal location at the focal point of a parabolic mirror.

To calibrate the WFS two independent 100 μR waveforms are required, with the tilts along the x- and y-axes. This requires source motion of about 540 μm along the x- and y-axes. The motion can be slow, around 1 Hz, so linear translation stages are appropriate to physically move the light source output. As described later, this is the output end of a fiber optic which conveys the beam from an external laser.

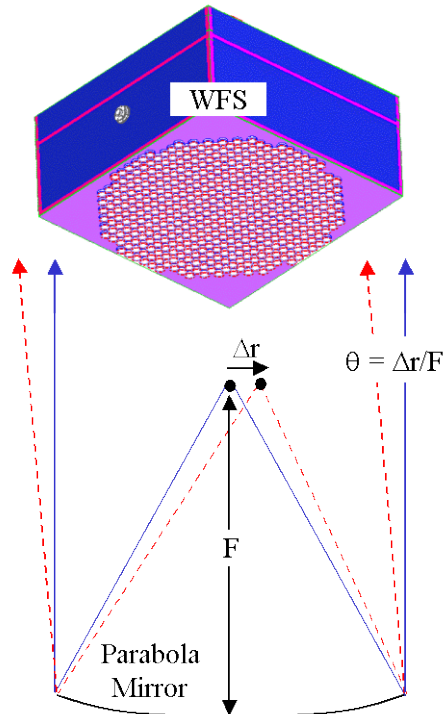


Fig. 1. The WFS test is achieved by moving the light source laterally about the parabola focal point, dynamically titling the collimated output beam. The wavefront slope is proportional to the source motion (Δr) and the focal length of the mirror (F).

For wavefront performance tests, input waveforms on the order of 100 nR are required. This would require $0.5 \mu\text{m}$ source motion, too small to be practical in this system. Instead, a fold mirror mounted on a PZT (piezo-electric transducer) is placed near the source. The PZT can tilt the mirror by very small amounts (a few μR) which moves the virtual source (the reflection of the source seen by the mirror). This is shown in See Fig. 2. For a rotation $\Delta\phi$ the virtual source rotates by twice that, $2\Delta\phi$. This causes a translation perpendicular to the output beam direction, given by $\Delta r = L \sin(2\Delta\phi) \approx 2L\Delta\phi$. There is also source translation Δz along the beam but it is negligible for small mirror tilts. A high resolution PZT actuator is used to tilt the fold mirror, and the distance L is chosen so that 100 nR of wavefront tilt is accomplished with $10 \mu\text{R}$ of fold mirror tilt. The beam path is then oriented so the wavefront tilt is along the WFS diagonal, providing 70 nR along both the x- and y-axes.

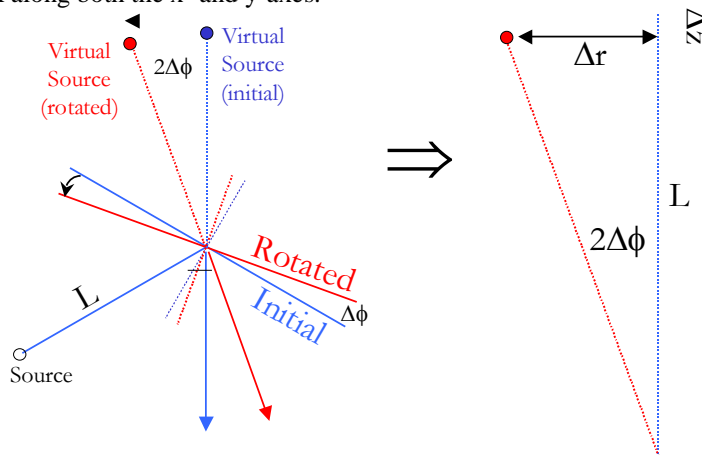


Fig. 2. Tilting a fold mirror causes translation of the virtual source (the reflection of the physical source). For small tilts, the virtual source motion is almost pure translation, relative to the initial reflected beam.

3. TEST IMPLEMENTATION

The schematic in Fig. 3 shows a diagram of the Parabola Assembly, while Fig. 4 shows the Assembly in the Test Chamber, underneath the WFS. The WFS is installed at the top of the test tower, supported by two rails. On the rails are a three-cylinder vibration isolation system. There is also a six-actuator motion positioning system for fine alignment.

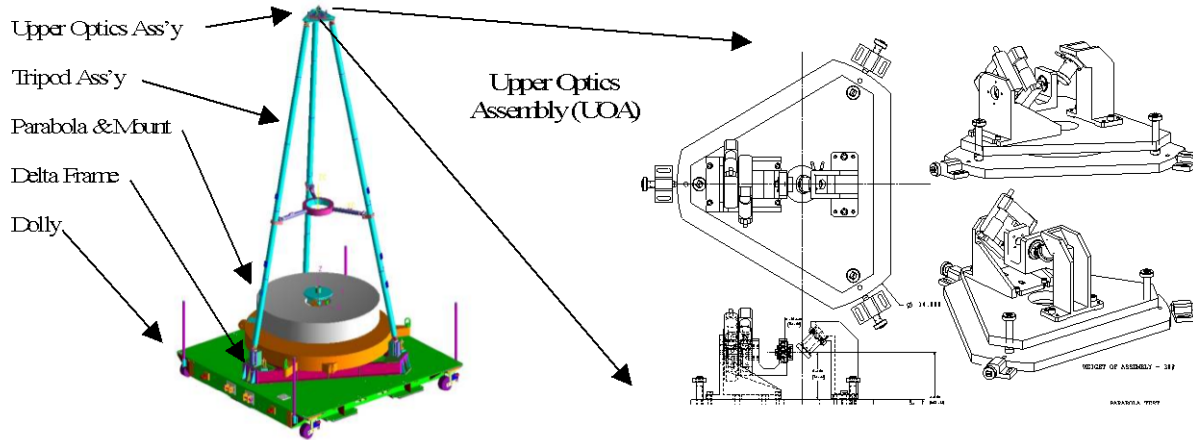


Fig. 3. Parabola Test Assembly with Details of the Upper Optics Assembly.

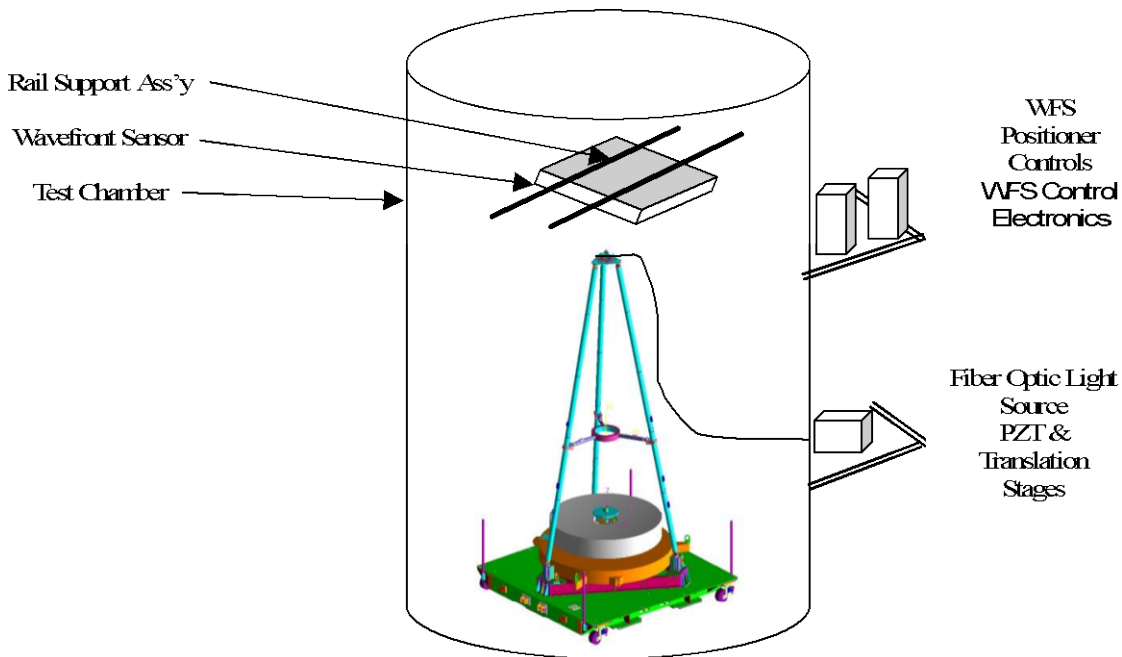


Fig. 4. WFS test assembly inside chamber, below the Wavefront Sensor.

The upper optics assembly (UOA), shown in Fig. 3 and Fig. 5, was used to calibrate the WFS and generate the tilt signals for testing. A 50 mW laser diode source at 0.852-micron wavelength (infrared) is located outside the test chamber. It is launched into a 20-meter fiber cable, which goes through a chamber penetration plate. The output end of the fiber optic cable is located at focal point of the parabola mirror (at the UOA). The fiber source output is expanded by a small lens to match the F/no of the parabola. After reflection downward by the PZT mirror, the parabola reflects and collimates the light, directing it upward to the top of the test chamber. The WFS, at the top of the chamber, faces the parabola and receives a full aperture beam.

The UOA, located at the focal point of the parabola, contains the PZT / mirror assembly and two translation stages. Translation stages move perpendicularly to the optical axis. These stages are used to calibrate the WFS system. One at a time, each decenters the source point in the parabola focal plane at 1/2 Hz, first in X and then in Y, creating 100 micro-radians (μR) of wavefront tilt in each axis. This process sets the WFS software constants which are later used to report absolute tilt values on each of the 448 sub-apertures.

After WFS calibration the stages remain fixed while the PZT is turned on. It oscillates sinusoidally in a tilt mode, creating a translation of the reflected image of the optical source inducing wavefront tilt at the WFS. The PZT mirror is oriented so that equal tilt values are created simultaneously along the X and Y axes. The PZT frequency and amplitude are independently adjustable, with a frequency range of approximately 10 to 200 Hz, and the amplitude range of approximately 10 nR (P/V) to 100 nR (P/V).

The true value of tilt is established through independent calibration of the PZT and determination of the exact spacing between the source and PZT mirror. This is used to verify the WFS's ability to measure tilt values in the desired operating range. The PZT was characterized up to a maximum of 50 Hz prior to the test, as we anticipated using only low frequencies. This calibration will be repeated for the higher frequencies that we used in the test (up to 315 Hz) due to the need to avoid the unexpected seismic disturbances.

The test processes take place in a vacuum chamber to remove the distorting effects of the air path. In the chamber, the 6-degree-of-freedom actuator system is used to point the WFS so that it is normal to the incoming wavefront within the capture range of the WFS of ± 4 milliradians. The isolator system contains 3 separate cylinders which, when filled with pressurized air, are designed to suppress seismic disturbances above approximately 1 Hz.

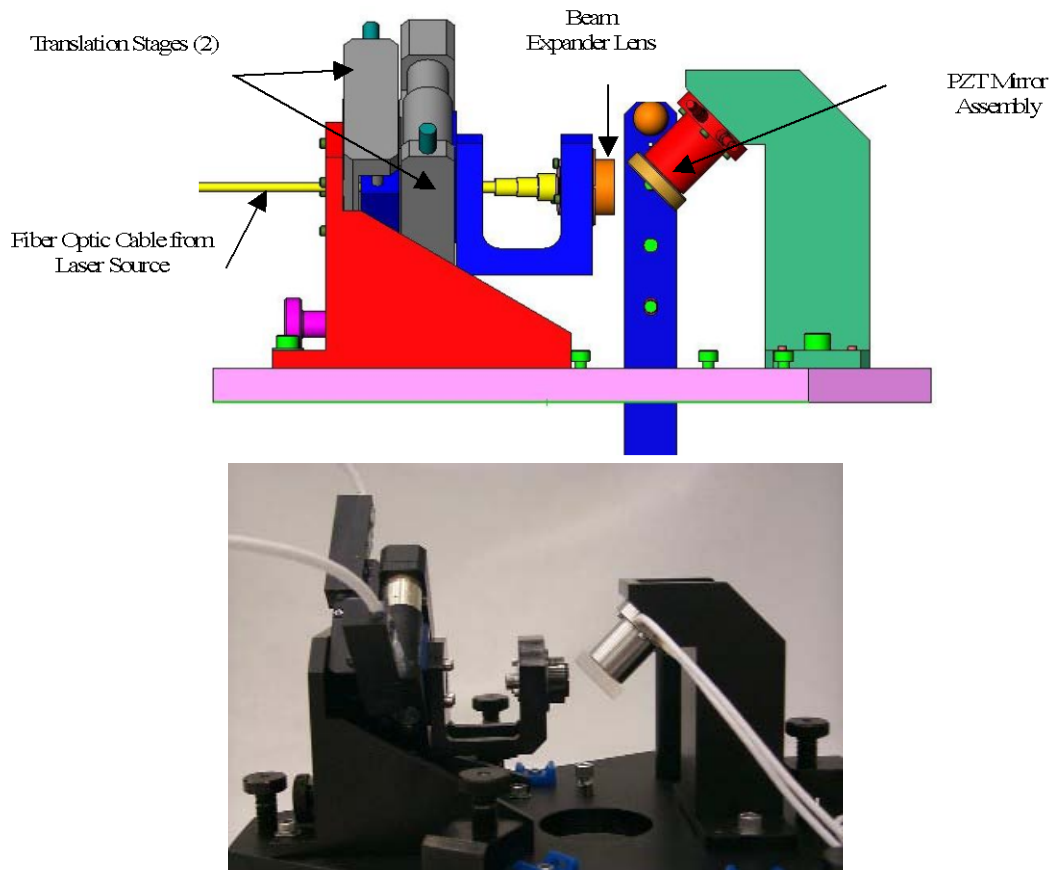


Fig. 5. Schematic of Upper Optics Assembly (top) and photograph of hardware (bottom). The translation stages, on the left, provide $540 \mu\text{m}$ of linear motion to steer the output beam during WFS calibration. The PZT tilts its attached fold mirror $10 \mu\text{R}$ to steer the beam for WFS tilt sensing testing.

4. WAVEFRONT TILT CALIBRATION

To create the necessary wavefront tilts during WFS testing, the translation stages and PZT in particular required characterization.

The translation stages were mounted in their WFS-test configuration. They were perpendicular to each other to provide x- and y-translation in the WFS test configuration coordinate system. A retro-reflector was mounted to the front stage, visible to a distance-measuring interferometer. Each stage was run through its calibration motion, a $\pm 272 \mu\text{m}$, $\frac{1}{2}$ Hz. trapezoidal pattern. Typical measurement data are shown in Fig. 6. Crosstalk was also measured, the x-motion during a y-translation and the y-motion during an x-translation, shown in shown in Fig. 7. The linear translation had a 2% RMS position error at the motion limits. The calibration data gave a 3° perpendicularity error between the translation stages.

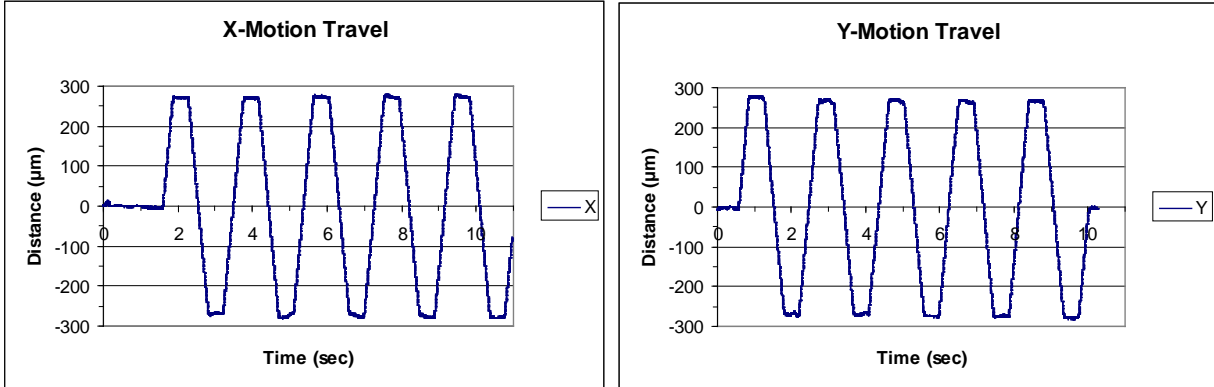


Fig. 6. Measured motion for front stage, for a $\pm 272 \mu\text{m}$ trapezoidal pattern

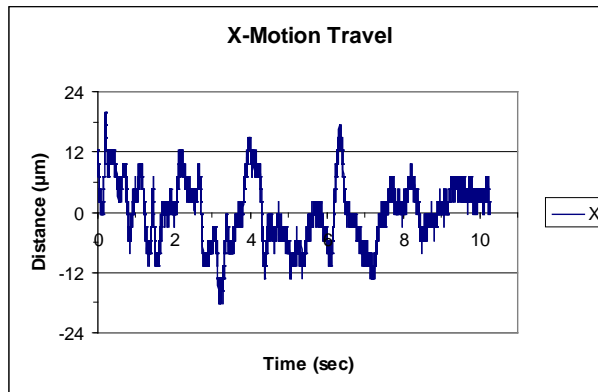


Fig. 7. Crosstalk along x-axis during y-translation measurement.

The PZT was calibrated using a laser vibrometer to measure real-time mirror displacement during tilting. The relative position of the mirror face was fit to a parabola at each sample for various sample times. The fit coefficients' variations were then fit to sinusoids over a single period. An example of this is shown in Fig. 8. The coefficient for vertical tilt b is divided by the mirror size to determine mirror tilt. The a coefficient is undesired tilt in the perpendicular direction; converting it to tilt gives the tilt error. Piston error c is ignored. Non-linear mirror motions, coefficients d and e represent measurement noise or micro-face motions that are also part of the error. See Fig. 9 for measured PZT tilts used in the WFS verification tests.

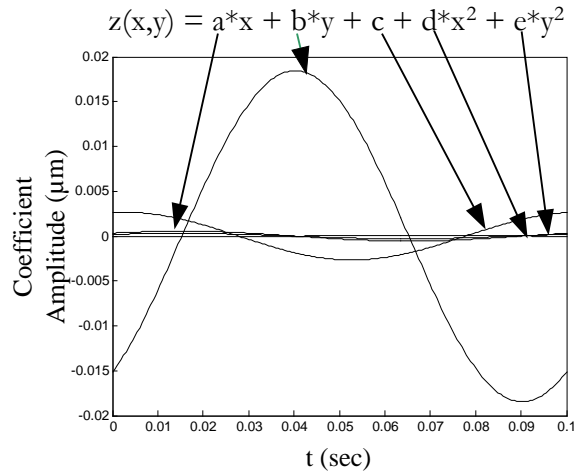


Fig. 8. Dynamic coefficients for one PZT test at 10Hz, equivalent to a 244 nR wavefront tilt. Ideally the b coefficient would be the only non-zero coefficient, reflecting pure vertical tilt.

PZT Calibration Data. Equivalent wavefront tilt (nR) for different oscillation frequencies.		
10 Hz	20 Hz	50 Hz
75.8 ± 0.4	67.0 ± 0.6	
121.6 ± 0.6	116 ± 1	
244 ± 1	234 ± 2	186 ± 8

Fig. 9. This table gives the PZT tilt as effective wavefront tilt (nR). It was found that for constant PZT inputs, the peak tilt decreased as frequency increased.

5. TEST RESULTS

The WFS measures the intensity of the wavefront-created fringe pattern on the four x-detectors and four y-detectors at each of the 448 sensors. This data is stored directly to the StreamStor device as raw data at 4000Hz. From the raw data the phases along the x- and y-axes are calculated and from that the x- and y-wavefront tilt. The computed x- and y-wavefront tilt data is decimated and analyzed within the WFS software at a user-defined frequency, 1000 Hz during this experiment. The wavefront tilt data can be examined during testing with the WFS control program and exported for offline analysis.

The wavefront tilt generally has an arbitrary bias level for each sensor that is constant for the sample time. With a view towards analyzing dynamic wavefront behavior this bias is irrelevant. Invalid sensors are then identified with typical results shown in Fig. 10. Any sensor with all zero wavefront tilt is considered “empty.” While this could be the result of a non-functioning sensor, as a rule it indicates an obstructed sensor, receiving no light, or poorly illuminated sensors at perimeter. Any sensors reporting invalid tilts (not-a-number (NaN)) are labeled “dead.”

Though the WFS software exports time-domain data, analysis is better done in the frequency domain since there harmonic test can be more easily distinguished from noise, as shown in Fig. 11. The power spectral density (PSD) of the wavefront tilts are computed and a representative few are displayed. The region of interest in the PSD is selected, shown in Fig. 12, such as the spike from the input test signal and the integration method chosen. The PSD data for all sensors is then processed and a series of graphs summarizing the data created.

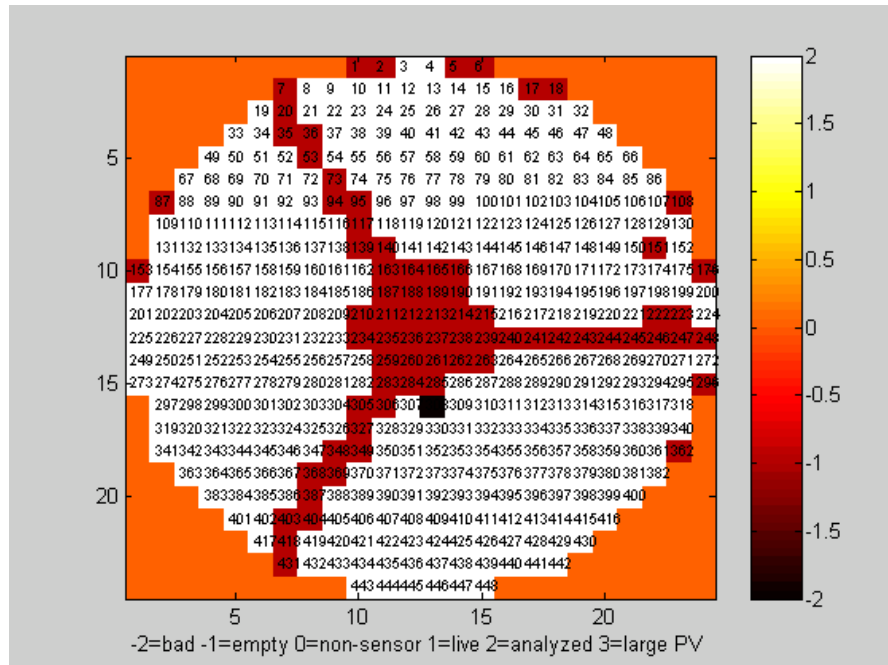


Fig. 10. WFS map with sensor numbers labeled. White are valid, analyzed sensors. Dark red are “empty” sensors reporting zero tilt at all times. Most empty sensors are those obstructed by test-set hardware (tripod & UOA) or are at the edge of illumination, though sensor 151 may be a failed sensor. The black square is a bad sensor and reports invalid tilts. And sensor 308 was dead for tests analyzed.

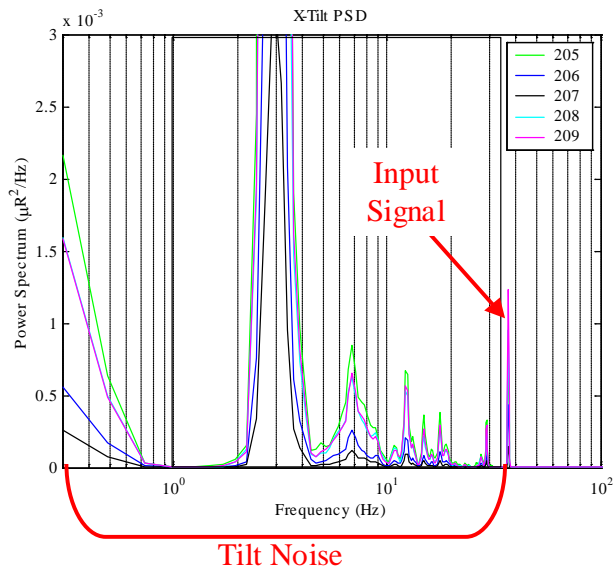


Fig. 11. Typical PSD curves from wavefront tilt data. Here the input signal was at 37 Hz and was the only optical signal. But environmental noise vibrated the WFS test equipment, causing mechanical tilts relative to the optical beam which were detected as optical tilts. The noise is primarily below 30 Hz but has significantly more energy than the test signal. Here, the test signal is a 35 nR RMS amplitude sinusoid and the total noise from 1 to 30 Hz is about 200 nR RMS.

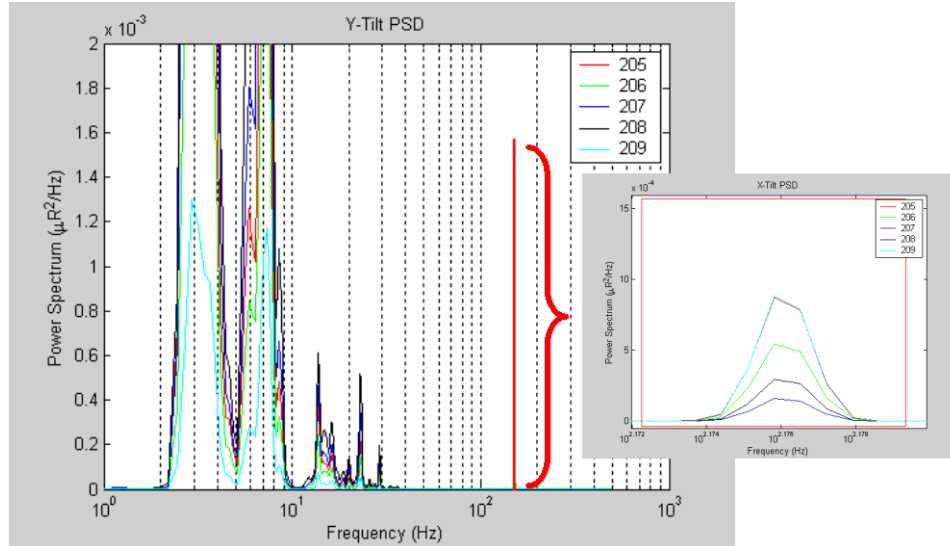


Fig. 12. Y-tilt PSD curve with 150 Hz test signal selected for analysis, highlight in red. The selected region is shown in the inset figure. Sinusoidal input signals have a Gaussian PSD form.

In exploring the data it was found that the PSD of a sinusoidal input signal has a Gaussian form, given in eq. 1. In that equation the Gaussian z has the parameters A for PSD amplitude, x_0 for frequency center, w as the width, and z_0 is the bias. And as PSD is energy squared per frequency, integrating it over some frequency range gives the mean-square (RMS^2) of the signal within that frequency range. For sinusoidal signals, the signal amplitude is proportional to the RMS, so measured signal amplitude can be calculated from its PSD, by $A = \sqrt{2} \cdot \text{RMS}$. Thus fitting the data from the measured input signal to a Gaussian and then analytically integrating was a fast and accurate means to calculate the measured wavefront signal amplitude.

$$z(f) = Z \exp \left[- \left(\frac{f - f_0}{w} \right)^2 \right] + C \quad (1)$$

Forty-one tests were conducted in January and February 2004. Because of pervasive environmental noise the best tests are considered to be from the late afternoon., as the area was generally quieter outside of normal work hours. These data sets were analyzed. Fig. 13 shows the measured PV signals with error bars. The mean signal amplitude reported agrees well with the input signals for all tests. X-Tilts are consistently reported about 30% higher than Y-Tilts. This suggests consistent clocking error in the test setup or a calibration error. The variation of the measured signal, however, is substantial with standard deviations of similar magnitude as the actual measured values.

Though the mean measured wavefront tilts were close to the input signal values, the RMS error was large. Examining the WFS calibration data it was found that the signal-to-tit gain values substantially varied from the nominal value. During normal operation these values should vary less than 1%. Analyzing the data for only those values for one data set, the results were much improved. For a 35 nR, 150 Hz input wavefront tilt, using only the best sensors, The median values were 34 nR and 28 nR and the RMS were 7nR and 17 nR for the x- and y-tilts, respectively. There were about 20 points for x and 10 for y. These results are shown in Fig. 14.

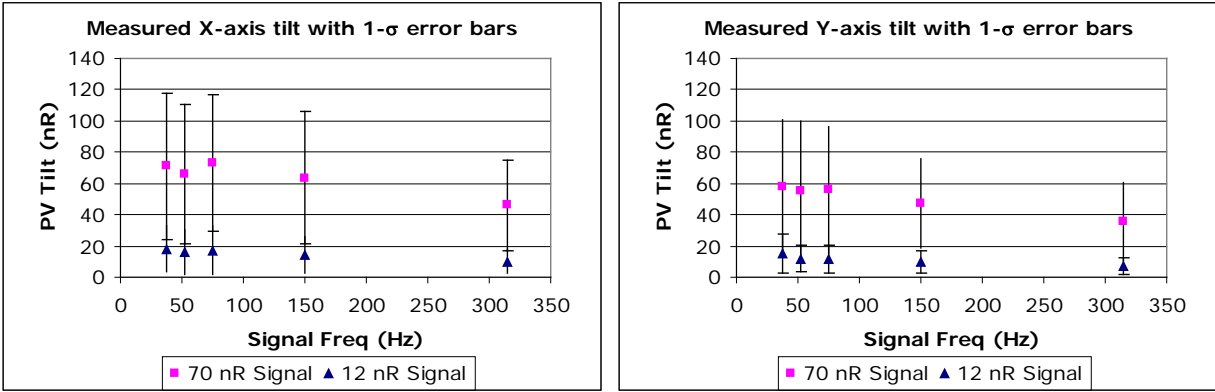


Fig. 13. Signal amplitudes with 1- σ error bars (\pm standard deviation). There is a trend downward in measured signal strength with increasing frequency for both directions and test amplitudes. This indicates the PZT travels less distance during high-frequency oscillations. Improved calibration would compensate for this behavior. The large error bars show the large variation in individual sensor measurements, though the mean detected signal is close to the actual input signal.

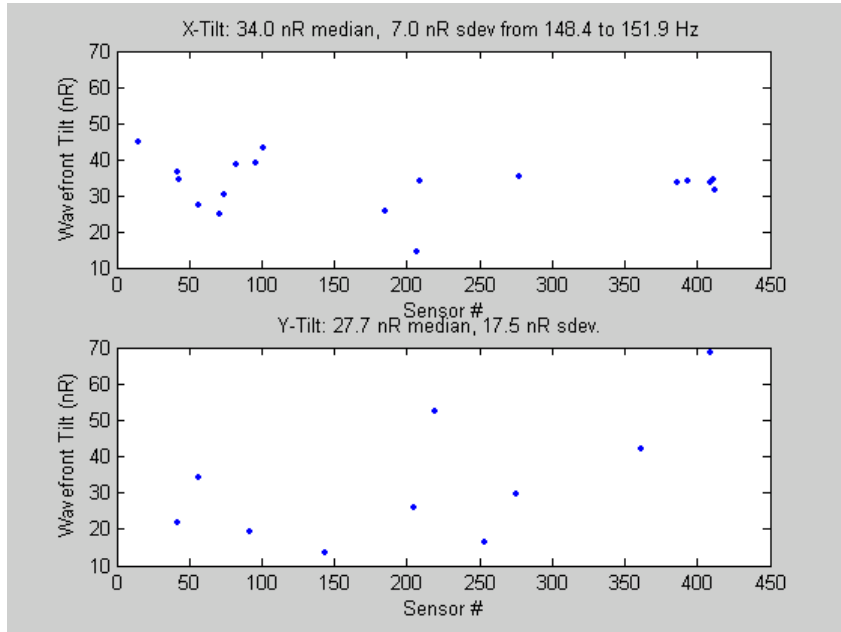


Fig. 14. Analysis of sensors with gain values within $\pm 1/2\%$ of nominal value. The error is reduced substantially.

6. SYSTEM IMPROVEMENTS

Since the original test, three major improvements actions have been performed. First, the isolation system, which failed during testing, has been repaired. This is expected to reduce the ambient seismic noise by a factor of eight. Second, an additional isolation system has been implemented to reduce noise from the parabola system. And third, the WFS alignment sensors were re-calibrated.

The coarse alignment sensors were found to be biased such that the WFS was actually mis-aligned to the just past the edge of capture range for most of the sensors. This, combined with seismic influences, are the likely causes for the wide data variation. As seen previously, for the few sensors properly in alignment, with good gain calibrations, the measurement performance was substantially better than the mis-aligned sensors.

7. CONCLUSIONS

The wavefront sensor has been analyzed for optical performance in the presence of high seismic vibration level. The results showed credible data consistency with the WFS seeing both a controlled calibrated optical disturbance from a full aperture parabola (37 to 315 Hz signals) and mechanically (seismically) induced optical beam disturbances from low frequency motions of the WFS and parabola. There were also observations and supporting analysis of resonances above 10 Hz due to the low frequency input energy.

Sinusoidal tilt signals of 70 nR (full range) at various temporal frequencies between 35 Hz and 315 Hz were clearly reported by the WFS. Input signals in the 12 nR range were also identified in the data. However, low frequency seismic disturbances, particularly in the 2 to 10 Hz range, created simultaneous tilt signals in the 100 to 1000 nR range, making it impossible to test the WFS to its performance limits. Attention of the seismic signals by at least 10X of the integrated signal from 2 to 10 Hz at both the WFS and the parabola is essential to being able to operate and test the WFS to its specifications. Further, the WFS alignment sensors were not calibrated and testing was likely performed at the edge of the sensors capture range, reducing measurement quality.

This test gave valuable insight into the WFS operation, the test environment and the support equipment in time to adjust, repair, and augment the components. A retest is planned for August, 2004, to determine the actual operational limits of the WFS and verify that all the necessary support equipment is working properly.

ACKNOWLEDGEMENTS

Many individuals of Harold Morris's project team assisted accomplishing these tests and then later in fixing the failed isolators. Larry Polsky and Bill Miller spent many hours analyzing seismic noise data in the weeks following test completion. Bill Jones, for his support and seasoned insights into calibration issues. And credit is due to the team at Optical Physics Company who both built the WFS and supported the test. We believe that it is realistic to expect exceptional performance during the next test.

REFERENCES

1. R. Hutchin, O. Otto, A. Wertheimer, *Design and Manufacture of a Large Aperture Wavefront Sensor*, companion paper 5553-25 in these Proceedings, 2004.

*david.fischer@kodak.com, phone 1 585 477 5814, fax 585-588-4939, address 800 Lee Road, Rochester, NY 14650-3118